Bicycle helmet design

N J Mills* and **A Gilchrist**
Metallurgy and Materials, University of Birmingham, Birmingham, UK

The manuscript was received on 20 March 2006 and was accepted after revision for publication on 31 July 2006.

DOI: 10.1243/14644207JMDA100

Abstract: Finite-element analysis (FEA) was used to consider the improvement of bicycle helmet performance, in oblique impacts with the road. The events, predicted by FEA, were described and the peak head accelerations interpreted in terms of a simplified model. FEA shows that thicker foam liners of lower compressive yield stress can protect the head against linear acceleration in 150 J impacts. The peak rotational acceleration of the head was shown to be only slightly affected by the friction coefficient on the road and, in general, to be insufficient to cause serious diffuse brain injuries. Improved protection of the forehead and temple was investigated; this required extending the liner downwards at the sides and front, and the inclusion of an oblique impact test in the BSEN 1078 standard.

Keywords: impact, FEA, bicycle helmet, foams

1 INTRODUCTION

If a cyclist is destabilized while riding and falls to the road hitting his or her head, the impact with the road surface will be oblique. Research on oblique impacts started in 1978, when Aldman *et al.* [**1**] dropped a complete, horizontally oriented helmet-wearing dummy, representing a motorcyclist, onto a rotating 1 m diameter table. More recently, finite element analysis (FEA) of oblique impacts on bicycle helmets [**2**] has been validated by comparison with experiments [**3**] for particular impact velocities. FEA is used here to consider helmet design, for a range of impact velocities.

The following four problem areas were considered. After briefly outlining the FEA method, the solutions are considered in turn.

1.1 Better protection in direct impacts

Can new designs, the use of novel polymeric foams, or multilayer foam mouldings, let cycle helmets protect against higher kinetic energy impacts normal to a rigid flat surface? The impact test energy in BSEN 1078 [**4**] is ~75 J (increasing with the headform circumference), equivalent to striking the road after a free fall from a typical riding height of 1.5 m. This is a common type of crash, typical when a glancing blow from a vehicle causes a cyclist to lose control. However, a rider who impacts a car windscreen may be projected higher into the air then fall to the road. If their helmet strikes part of a moving vehicle, the effective kinetic energy of the collision can also be larger. Henderson [**5**] wrote 'McIntosh and Dowdell [**6**] appear to have found no cases of helmeted cyclists surviving crashes where the equivalent impact velocity was greater than 20 km/h.' However, some Australian helmets from 1991 had 2 to 3 mm thick shells, whereas other had cloth covers ('soft shells'). They differed from those in 2006, which have circa 0.4 mm thick micro-shells, often bonded to the expanded polystyrene bead foam (EPS) liner. The vertical impact velocity in laboratory impact tests should not be confused with the total velocity of a cyclist. A BMA booklet [**7**] states: 'Cycle helmets are designed to protect the head during a low speed impact, e.g. 20 km/h, such as would occur in a fall to the ground from a bicycle. It is likely that most of the 183 UK cyclist deaths recorded in 1997 would have resulted from velocities and energies in excess of the average cycle helmet's ability to prevent the tragic outcome.' However, no research evidence is provided to support the second statement; the fraction of the 183 cyclists who wore helmets, or the crash circumstances, is not known.

**Corresponding author: Metallurgy and Materials, University of Birmingham, Birmingham B15 2TT, UK. email: n.j.mills@bham.ac.uk*

Downloaded from pil.sagepub.com at PENNSYLVANIA STATE UNIV on March 4, 2016

REVELYST 1032

A simple design process for direct impacts at a specified velocity [**8**] limits the impact force to 10 kN, hence limiting the head linear acceleration to ~200 g. It uses the relationship for the force F, acting towards the centre of gravity of the head

$$F = 2\pi R_{\mathrm{H}} \sigma_{\mathrm{y}} x \tag{1}$$

where σ_{y} is the constant yield stress of the foam, R_{H} the radius of curvature of the helmet outside at the impact site, and x the liner crush distance. The foam thickness is chosen so that the design impact energy is dissipated when the foam is nearly bottomed out, at ~90 per cent compressive strain. Equation (1) then gives the appropriate foam compressive yield stress. The polymer foam with minimum density for this yield stress is chosen to minimize the liner mass. It is assumed that the initial design just meets the 75 J kinetic energy requirement of BSEN 1078. Consequently, to protect the head against an impact energy of 150 J, the foam liner must be twice as thick and the foam yield stress halved. However, any disadvantages of such designs for lower energy impacts must be considered.

A US patent [**9**] refers to papers [**10**, **11**] on the impact performance of high density polyethylene (HDPE) foam. It shows how a helmet, with a 20 mm layer of HDPE foam of density 80 kg/m^3 outside a 10 mm layer of HDPE foam of density 60 kg/m^3, could meet the 100 J impact test in the Consumer Product Safety Commission 1999 Standard for bicycle helmets. The German company ABUS introduced in 2005 a dual-density EPS bicycle helmet; it consists of two EPS mouldings, bonded together, with the denser moulding on the outside, creating complex-shape ventilation holes. However, densities (measured as 92 and 82 kg/m^3) do not differ sufficiently to greatly affect the mechanical properties. The Bicycle Helmet Safety Institute (www.bhsi.org) mentions new foams for helmets in its annual review of new helmets; some of these could have advantages over EPS.

1.2 Reduced head rotational acceleration in oblique impacts

Can the peak rotational head acceleration be reduced from the values typical for BSEN 1078 helmets, for impacts oblique to the road surface? An easy-shear interface between the shell and the liner of an open-face motorcycle helmet [**12**] was evaluated using an Ogle headform (6 mm of plasticized PVC over a hollow aluminium casting) that exactly fitted the motorcycle helmet liner with no comfort foam. With no rotation at the headform/helmet liner interface, the benefits of the easy-shear layer in reducing the head rotational acceleration may have been exaggerated. The micro-shells of most bicycle helmets partly enter the liner ventilation holes, so even if not bonded to the liner, cannot slide over the liner outer surface. Research [**13**] showed that jockey's heads, when they hit a racetrack, slid along the grass. Phillips patented [**14**] a low friction layer with a rubber cover for the outside of motorcycle helmets. A similar design on a bicycle helmet could possibly reduce the headform rotational acceleration. The criterion for the onset of diffuse brain damage is a rotational acceleration exceeding 10 k rad/s^2 [**15**].

1.3 Extended coverage of the head

Can greater protection be provided for the forehead and temple, compatible with vision, hearing, and comfort? Depreitere *et al.* [**16**] suggested that head coverage should be reconsidered; they found that 57 per cent of impacts occurred at the side and 27 per cent at the front of the head, and that the lower parts of these areas are not covered by current bicycle helmets. Current cycle helmets do not come down to the ear at the side of the head, and do not cover parts of the temple area. The '*Restriction of hearing*' clause in the obsolete BS 6863:1987 [**17**] standard prohibited any part of the helmet coming within a 65 mm diameter cylinder centred on the ear. However, it was never established that helmet intrusion in this region restricted hearing. In a fall to the side, the cyclist's shoulder usually hits the road before the head, reducing the head velocity and restricting the helmet sites that can be hit. It is not clear whether helmet liners provide significant protection for impact sites at their lower edge; the helmet may be displaced, or rotated on the head, in the impact. The brain injury threshold, for head linear acceleration in the ear-to-ear direction, appears to be lower than that for the nose-to-rear direction [**18**]. If EPS helmet liners cover more of the head, a greater range of helmet interior shapes and sizes are necessary to fit the range of head shapes and sizes in the population. The Sportcraft helmet [**19**] consists of six EPS segments held together with embedded polymer netting strips; the five side segments are pulled into contact with the sides of the head by tightening the retention webbing, overcoming the necessity of manufacturing a range of liner shapes.

1.4 Problems with current foams

Burdett [**20**] argued that vents in cycle helmets lead to excessive pressures on the skull. However, there are no reported cases of scalp bruising from the use of cycle helmets, or of skull fractures due to localized loading. Aldman [**21**] stated that a depressed skull fracture was likely in the temporal area if a pressure of >4 MPa acted on an area < 5 cm^2. As most of

Downloaded from pil.sagepub.com at PENNSYLVANIA STATE UNIV on March 4, 2016

the skull bones covered by helmets are stronger than the temporal bone, depressed skull fractures are not expected for pressures <5 MPa. Burdett [**20**] also argued that 'the helmet's liner is made of stiff foam and requires a certain minimum force before it starts to crush. Until this minimum is reached, the head must absorb the impact. This means that, although helmets are designed to limit the impact (deceleration) to a just sublethal level, they would not reduce it much below that. In these cases, sublethal translates into anything from a very bad concussion to a coma.

Although epidemiological studies [**22**] show the effectiveness of helmets in reducing the number and severity of bicyclists' head injuries, some critics argue against helmets. They may start with a false premise, that most injuries are due to rotational head acceleration, then argue that helmets do not reduce rotational acceleration. Curnow [**23**] claimed that, since epidemiological studies do not distinguish between skull fractures and injuries caused by angular acceleration, they do not demonstrate the efficiency of helmets in preventing head injury. This area needs clarification.

2 OUTLINE OF THE FEA METHOD

Details of the FEA are provided in reference [**2**]. This was validated by comparing predictions of linear acceleration traces, normal and tangential forces on the road surface, and predictions of helmet rotation with experimental data [**3**]. The geometry and meshing of the four main bodies are summarized here for convenience.

2.1 Helmet liner

Dr Brühwiler of EMPA, St Gallen, Switzerland, kindly provided the scanned shapes of a Specialized S1 bicycle helmet with a 230 mm internal length, and a headform. The helmet liner shape was reduced to 2500 triangular facets and an ACIS .sat file imported to ABAQUS as a three-dimensional solid part. The liner thickness was 24 mm at a frontal site and 21 mm at a lateral site (both 70 from the crown).

A smooth surfaced helmet, with 16 holes and a nearly uniform liner thickness of ~28 mm, was drawn using a CAD package. It lacks the internal fore-and-aft air-flow grooves of the S1 helmet, but covers slightly more of the head.

2.2 Shell

The outer part of the three-dimensional liner was converted to a shell, with its edge at the location of the real helmet shell edge. It was assigned a Young's modulus of 3 GPa, a Poisson's ratio of 0.4, and an initial tensile yield stress of 60 MPa, which increases to 70 MPa at a strain of 1.0, data typical for polycarbonate. It was 0.4 mm thick, typical for bicycle helmets, and it was tied to the liner exterior surface to simulate the 'in-mould' bonding process.

2.3 Headform

Hollow aluminium headforms are used for EN 1078 helmet testing. Their moments of inertia are based on measurements with cadaver heads on a torsion pendulum at a frequency of ~1 Hz, so the soft tissues do not deform. The scanned headform was scaled to have a length (Table 1) similar to the test headform. It was modelled as a rigid shell, with a mass (4.26 kg) and moments of inertia equal to those of the test headform. A three-dimensional deformable headform was used for one simulation to show surface pressure contours. FEA showed that its peak linear acceleration was within 1 per cent of that of the rigid headform, for the same impact conditions and helmet.

2.4 Retention straps

15 mm wide side, chin, and nape straps were positioned at ~5 mm from the headform. They were meshed with linear triangular membrane elements M3D3. The Young's modulus was 1.0 GPa and the thickness 1.3 mm, providing a tensile stiffness of 18 kN, equal to that measured for polyethylene terephthalate webbing. A separate FEA was made of jerking the strap ends upwards, then an orphan mesh taken from the results file when the strap tensile stresses reached 10 MPa. This closely followed the headform surface and was used as a stress-free part in the main FEA. Nodes on the straps, 50 mm above the lower edge of the helmet, were tied to the liner inner surface to provide mountings.

2.5 EPS foam model

The Crushable foam model in ABAQUS is for isotropic materials that harden as the volume changes. A

Table 1 Headform dimensions, masses, and moments of inertia

Headform	Circumference (mm)	Length (mm)	Breadth (mm)	Mass (kg)	I_{xx} (kg cm^2)	I_{yy} (kg cm^2)	I_{zz} (kg cm^2)
Test	580	190	158	4.26	199	237	172
Used in FEA		199	154	4.26	192	240	163

Downloaded from pil.sagepub.com at PENNSYLVANIA STATE UNIV on March 4, 2016

previous publication [**24**] described its use for EPS. The EPS had an initial yield pressure in hydrostatic tension $p_t = \sigma_{C0}$ and the initial yield pressure in hydrostatic compression $p_{C0} = 0.517\sigma_{C0}$, where σ_{C0} is the initial uniaxial compression yield stress. The yield surface is determined from these three stresses. The post-yield hardening of EPS in uniaxial compression was described by

$$\sigma_C = \sigma_{C0} + \frac{P_0 \varepsilon}{1 - \varepsilon - R} \tag{2}$$

where ε is the strain, P_0 the effective gas pressure in the undeformed cells, and R the foam relative density (the EPS density divided by the 1050 kg/m^3 density of solid polystyrene). Table 2 gives the data for the foams simulated.

2.6 Contact conditions

There was a 3 or 4 mm gap between the headform and the liner interior surface at the start of the simulations; in the real helmet, there are pads of soft polyurethane open-cell (comfort) foam in this space.

The coefficient of friction at the head/liner interface was 0.6, whereas that at the shell/road interface was 1.2. The maximum shear stress was 0.5 MPa at the head/helmet interface and 5 MPa at the helmet/road interface, whereas the 'shear traction stiffness' of the interface was 5 and 50 MPa, respectively. Elastic slip was allowed with an elastic shear stiffness 10 times the shear stress limit. These parameters gave the best correspondence with data from laboratory oblique impact tests [**2**]. A nonlinear stiffness function was used normal to the contact surfaces, with a pressure of 100 MPa to cause an over-closure of 1 mm. The over-closure in the simulations was of this order, so reasonable.

2.7 Meshing and impact simulations

The parts were seeded at 8 mm spacing. The specialized helmet had 7943 elements in the liner, 2274 in the shell, 2562 in the headform, and 397 in the strap system. The liner was meshed with modified 10-node quadratic tetrahedral elements C3D10M, the rigid headform with linear rigid triangular R3D3 elements, and the shell with linear triangular shell elements S3R.

Table 2 Properties of EPS

Density (kg/m^3)	Young's modulus E (MPa)	Poisson's ratio	Initial yield stress σ_{C0} (MPa)	Effective gas pressure P_0 (MPa)
35	10	0.1	0.29	0.15
55	20	0.1	0.6	0.20
83	40	0.1	1.10	0.27

Explicit FEA was used with ABAQUS version 6.5. Figure 1 shows the *xyz* axes through the headform centre of gravity and the 123 axes of the road. The headform and helmet always had its tangential impact velocity component V_T along the 3 axis and normal component V_N along the 2 axis. The helmet position relative to the road was described by the rotation angle and direction (left, front, etc) from the crown-to-road position; after the rotation, the helmet and headform were moved along to the 2 axis to just touch the road.

2.8 Impact forces and head accelerations

It is difficult to explain the complex events of helmet oblique impacts and peak head acceleration levels, in terms of a simple model having a few mechanisms. Useful simplifications are to treat the head as a rigid mass and to ignore the helmet mass in comparison with the headform mass. The crushed foam approximates to a thin layer, in the 1, 3 plane (Fig. 1). By Newton's second law

$$F_N = ma_N \tag{3}$$

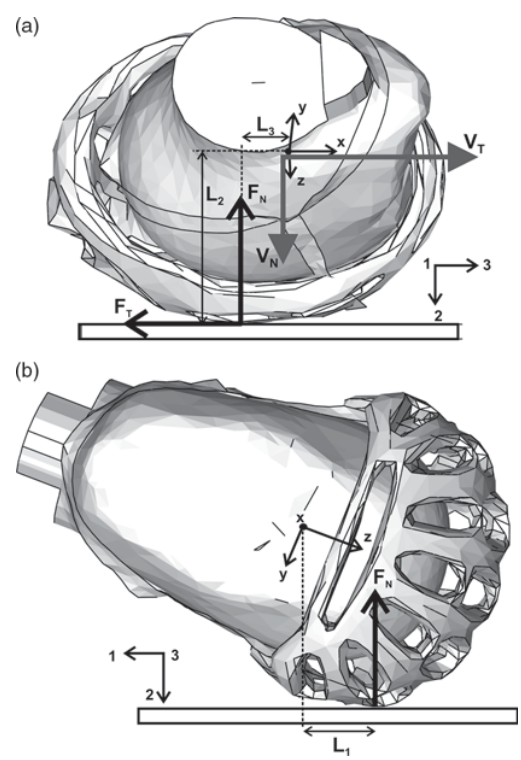

Fig. 1 Oblique impact on the left 70° site of a S1 helmet, showing the axes *xyz* through the headform centre of gravity and road axes 123. L_i are the offsets of the lines of action of the normal F_N and tangential F_T forces from the headform centre of gravity

Downloaded from pil.sagepub.com at PENNSYLVANIA STATE UNIV on March 4, 2016

the head linear acceleration a_N is proportional to the impact force F_N normal to the road and inversely proportional to the head mass m. The impact force component F_T acts tangential to the helmet surface, hence tangential to the head surface. The rotational equivalents of Newton's second law for the head are, for the 1 and 3 axes of rotation shown in Figs. 1(a) and (b) are

$$L_2F_T + L_3F_N = I_1\ddot{\theta}_1$$
$$L_1F_N = I_3\ddot{\theta}_3 \quad (4)$$

I_1 and I_3 are the head moments of inertia about the appropriate axis, whereas the lines of action of the force components are offset from the head centre of gravity by L_i. Hence, the head angular acceleration $\ddot{\theta}_3$ is initially proportional to F_N for the impact site shown in Fig. 1(b). However, as the helmet rotates on the road, the L_i change and the equivalents of equation (4) become more complex.

The tangential force, produced by friction at the helmet/road interface, is restricted in magnitude by slip at the head/helmet interface. This, and the helmet's low moment of inertia, mean is that the effective friction coefficient of the helmet/road interface is about 0.2 [**3**].

3 INCREASING PROTECTION LEVELS FOR LINEAR ACCELERATION

3.1 Thicker liners

The simulations used the 16-hole helmet with a 28 mm thick liner of EPS with density 55 kg/m^3. Figure 2(a) shows the variation of the normal force F_N from the road versus x, the reduction in thickness of the liner at the centre of the impact region (measured from the closest distance between the headform surface and the road), for an oblique impact on the right hand 70° site with $V_N = 8.39$ and $V_T = 10$ m/s. When $V_N = 8.39$ m/s and $V_H = 0$, the impact kinetic energy is 150 J, the target value. The increase in F_N with x is initially almost linear, in agreement with the simple theory of equation (1) and with prior FEA simulations [**3**]. However, towards the peak of the impact, a large ventilation hole rotates into the middle of the crushed region (Fig. 2(b)), reducing the value of F_N. The impact at the left 70° site causes the region of crushed foam to extend to the lower edge of the helmet. It is beneficial to have no ventilation holes in this region to increase the amount of foam that is crushed.

Table 3 gives the peak head accelerations for a range of impact sites. For the side and crown impact sites, the horizontal velocity component beneficially decreases the peak linear head acceleration, due to the rotation of uncrushed foam into the contact region. Its effect on the peak rotational acceleration is neutral, with an increase in the 1 axis component and a decrease in the 3 axis component. The peak rotational accelerations are low for the crown site, since the offsets L_1 and L_3 of the impact force F_N are relatively small. For the impact on the front 90° site, the chin of the headform just hits the road when $V_H = 5$ m/s, adding ~60 g to the peak linear acceleration, but doubling the peak head rotational acceleration, compared with the run when $V_H = 10$ m/s, in which there is no chin to road contact. In the latter, helmet forward rotation on the head ceases when the helmet brow wedges over the headform nose region, causing a peak in the headform rotational acceleration late in the impact. Whether the chin contacts the road depends on the

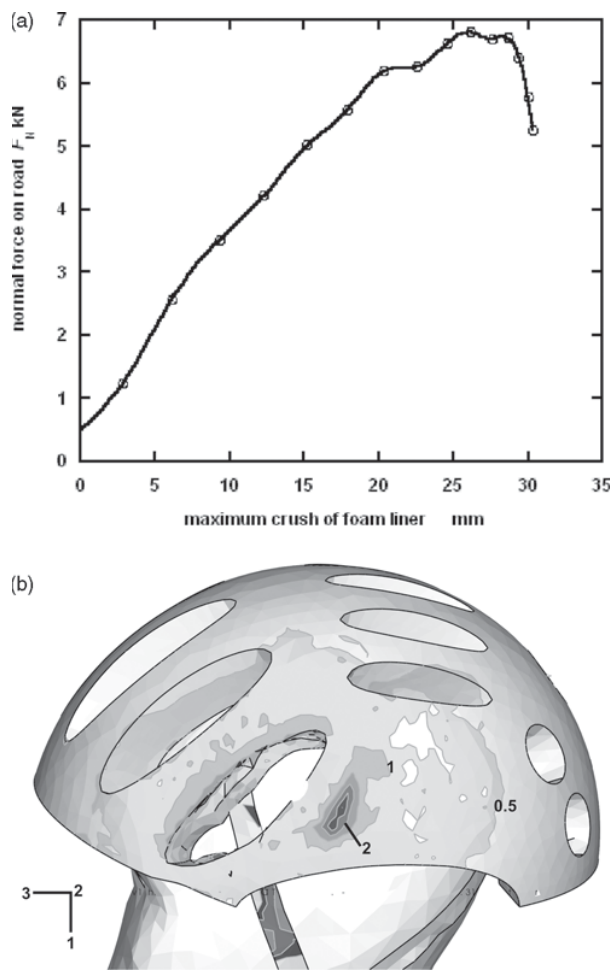

Fig. 2 Impact of 16-hole helmet with $V_N = 5$ and $V_T = 10.0$ m/s on the left 70° site: (a) variation of the normal force F_N with the foam crush distance in the centre of the impact region, and (b) contours of pressure σ_{22} (MPa) on the liner at the peak of the impact

Downloaded from pil.sagepub.com at PENNSYLVANIA STATE UNIV on March 4, 2016

Table 3 Predictions for the 16-hole helmet with EPS liner of density 55 kg/m^3

Impact site, direction, velocity V_N	V_H (m/s)	F_N maximum (kN)	F_T maximum (kN)	Minimum liner thickness (mm)	Head a_{max} (g)	Head $\ddot{\theta}_1^{max}$ (k rad/s^2)	Head $\ddot{\theta}_2^{max}$ (krad/s^2)	Head $\ddot{\theta}_3^{max}$ (krad/s^2)
Front 90°	10	3.80	2.06	7.0	98	7.9	0.1	0.1
Down	5	6.15	−1.15	9.8	160	15.8	0.5	0.5
6.0 ms^{-1}	0				chin strikes the road after 8 ms			
Side 70°	10	6.84	1.44	1.5	174	−8.7	−1.3	6.1
Back	5	8.47	1.30	3.0	209	−8.7	−1.0	7.7
8.39 ms^{-1}	0	9.61	−0.44	3.5	233	−5.6	0.8	8.9
Crown	10	8.15	3.60	6.3	208	4.0	0.7	0.9
Forward	5	8.56	2.42	6.7	208	2.0	0.5	0.8
8.39 ms^{-1}	0	9.60	0.53	7.2	231	−3.1	−0.6	0.8

initial orientation of the face relative to the road and the attitude of the helmet on the headform.

Thus, this helmet design, with some modifications in the ventilation holes, should pass 150 J impacts at a range of sites; in general, the foam is nearly bottomed out at its peak deformation. The foam thickness had been increased by ~27 per cent and its density decreased by ~34 per cent compared with the specialized helmet. Greater changes would maintain the safety margin for passing the impact tests. Although simulations of kerbstone impacts were not performed, it is likely that this helmet design would pass at the reduced velocity of 4.57 m/s used in BSEN 1078. FEA predicts that the long thin blocks of EPS, separating the long ventilation slots towards the front of the helmet, can move apart laterally during compression. It is important to prevent the EPS sections bucking, bending laterally, or rotating, in ways that reduce the energy absorption.

3.2 Novel foams

Foamed copolymers of ethylene and styrene (ARCEL from Nova Chemicals) and styrene–ethylene interpolymers (Dow chemical) have greater toughness and greater recovery after impact, than EPS of the same density. However, Masso-Moreu [**25**] found that these foams had a lower initial yield stress than EPS of the same density. Consequently, in terms of yield stress divided by density, they were inferior to EPS. Furthermore, the foams are considerably more expensive than EPS. As helmet should be destroyed after an impact, there is no need for a multi-impact product.

Brock foams, consisting of EPP beads adhesively bonded together, were investigated [**26**] because they offer the possibility of ventilation plus energy absorption. The approximately 0.25 volume fraction of air channels in these foams allows them to transmit water easily. However, their energy absorption efficiency was inferior to EPS, because their compressive stress–strain response was almost linear, whereas EPS has an initial yield stress followed by a lower slope during crushing. Therefore, at present, EPS seems to be the best material for the foam liner of bicycle helmets.

If lower-than-usual density EPS is used, it may be necessary to incorporate a high tensile strength structure, in order to retain reasonable tensile strength. The EPS can be in-mould bonded to the microshell or moulded around an internal tensile structure. Such structures are relatively common.

3.3 Two-foam helmets

To evaluate two-foam helmets, the 16-hole helmet design was fitted with two liner layers, each of thickness ~14 mm. In one version, a 35 kg density EPS inner liner was used with a 83 kg/m^3 density outer liner, and in a second version, 55 kg/m^3 density EPS was used for both liners. Figure 3 shows the liner deformations 3.6 ms after the start of an oblique impact with $V_N = 5.4$ and $V_T = 5.0$ m/s. In the first case, the inner liner is fully crushed at the centre of the impact site, whereas in the second case, there is nearly uniform deformation through the liner thickness. The peak head acceleration (Table 4) is lower for the uniform density liner, with more liner left uncrushed at the peak of the impact, than for the dual-density liner, so the former has a better performance and could cope with higher energy impacts. When a 35 kg/m^3 density liner was used on the outside, the simulation became unstable before the expected force peak. These limited simulations suggest that a dual-density liner is unlikely to have significant advantages over a single-density liner. However, denser foam could be used near the lower edge of the helmet, to compensate for the smaller contact area that occurs for low impact sites.

4 HEAD ROTATIONAL ACCELERATION IN OBLIQUE IMPACTS

4.1 Events in oblique impacts

The specialized helmet geometry was used for the majority of the simulations. Finite-element

Downloaded from pil.sagepub.com at PENNSYLVANIA STATE UNIV on March 4, 2016

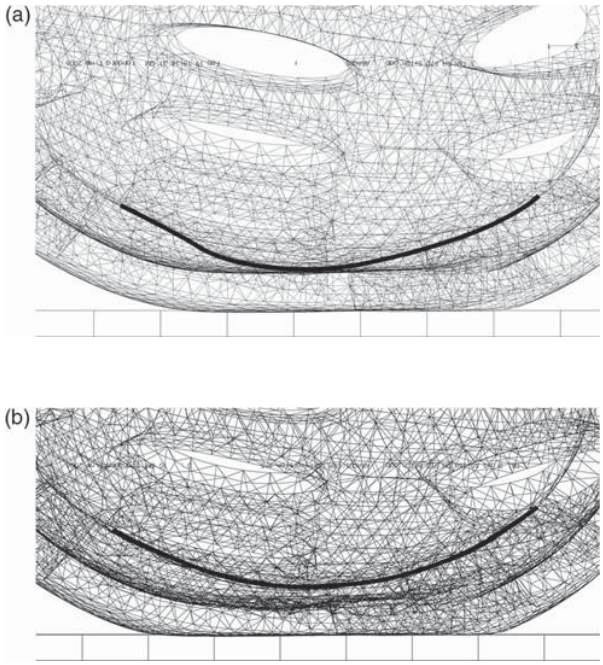

Fig. 3 Wireframe views in the 2, 3 plane of two-layer helmet liners after 3.6 ms, for impacts with $V_N = 5$ and $V_T = 10.0$ m/s on the left 70° site: (a) inner 35 kg/m^3 density liner and outer 83 kg/m^3 liner, and (b) two liners of 55 kg/m^3 density (inner surface of inner liner is emphasised)

modelling of helmet oblique impacts shows a complex series of events, involving a number of deformation mechanisms. In Fig. 4, marks on the head, helmet, and road emphasize the relative motion. The events are as follows.

1. From 0 to 1 ms, the internal pads of comfort foam compress, so the headform moves into contact with the inside of the helmet liner. The shell slides on the road surface.
2. From 1 to 5 ms, the liner foam compresses (crushes), and a 'flat' develops on its outer surface. The helmet shell ceases to slip and begins to roll on the road. For lateral impact sites, the helmet appears to act as a deformable 'roller' of near constant thickness, sliding at the head/helmet interface while rolling on the road. Figure 4(a) is at 1.8 ms just after the shell starts to roll. By 4 ms (Fig. 4(b)), the liner has crushed considerable. The 'flat' on the outside of the helmet hinders rotation, but slip occurs at the head/liner interface where the wearer's hair acts as a low-friction layer.
3. From 5 to ~10 ms, the liner foam partly recovers as the headform moves away from the road. There is more rotation of the helmet on the head, seen by comparing Fig. 4(c) with 4(d). By 7.8 ms (Fig. 4(d)), the helmet has rotated by ~15° relative to the head's neck to crown axis.

Figure 5(a) shows the time variation of the normal force F_N and tangential force F_T on the road surface and the major headform accelerations; its linear acceleration a_N normal to the road and its angular acceleration $\ddot{\theta}_1$ about the 1 axis (Fig. (1)). If F_N is plotted against a_N, the correlation coefficient $R = 0.999$ and, from the slope, the effective mass of the headform is 4.31 kg (in reality, it is 4.26 kg, while the helmet mass is 0.12 kg). However, the correlation of F_T with the angular head acceleration $\ddot{\theta}_1$ is poor (Fig. 5(b)). The peak headform rotational acceleration of 6.6 k rad/s^2 about the 3 axis is almost as great as the 8.2 k rad/s^2 about the 1 axis (perpendicular to the impact velocity plane). The peak normal force F_N of 6.89 kN is 6.0 times as great as the peak F_T and its line of action does not run through the headform centre of gravity. Hence, F_N affects the headform rotational acceleration as much as does F_T.

4.2 Effect of low-friction layers on head rotational acceleration

To assess whether low friction layers, either outside or inside the helmet, might reduce the head rotational acceleration, FEA simulations were made of low friction interfaces on the S1 helmet. Starting with the friction coefficients used to match experimental data (first row of Table 5), the values were progressively reduced. A reduction in the friction coefficients by a factor of 8 had little effect on the peak rotational accelerations; the shear stress limits were kept constant at 0.5 MPa for the road/shell interface and 5 MPa for the head/liner interface for these simulations. When the friction coefficients

Table 4 Peak headform accelerations for 16-hole helmet, having two EPS liner layers, for oblique impact on the right 70° site with $V_N = 5.4$ and $V_T = 5.0$ m/s

Inner liner density (kg/m^3)	Outer liner density (kg/m^3)	F_N max (kN)	F_T max (kN)	Min. liner thickness (mm)	Head a_{max} (g)	Head $\ddot{\theta}_1^{max}$ (k rad/s^2)	Head $\ddot{\theta}_2^{max}$ (k rad/s^2)	Head $\ddot{\theta}_3^{max}$ (k rad/s^2)
83	35	6.31	0.97	11.5	156	−5.8	−2.1	6.1
55	55	5.34	0.91	13.7	131	−4.8	−1.8	4.9

Downloaded from pil.sagepub.com at PENNSYLVANIA STATE UNIV on March 4, 2016

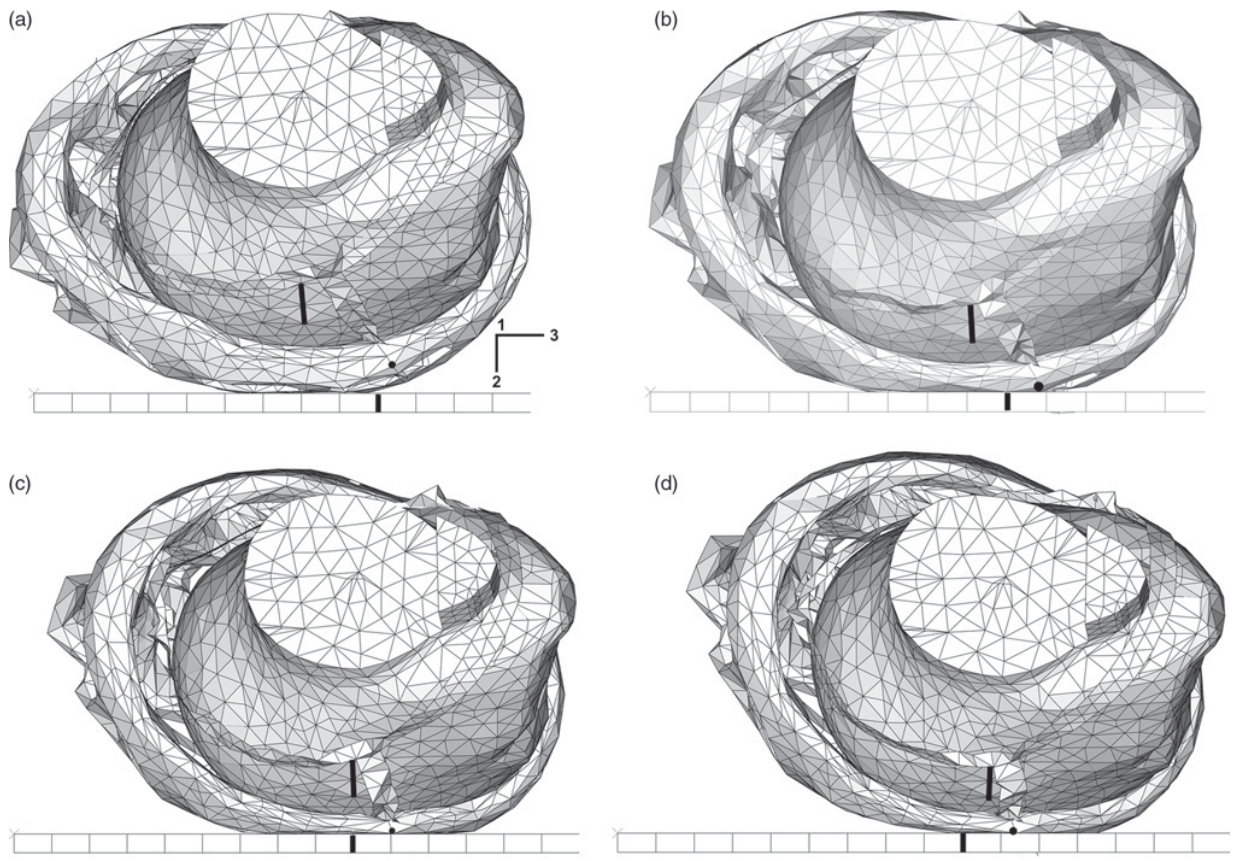

Fig. 4 2, 3 plane view of a S1 helmet oblique impacted on the left 70° site, with velocity components $V_N = 5.4$ and $V_T = 10.0$ m/s, at times: (a) 1.8 ms, (b) 4.0 ms, (c) 6.0; and (d) 7.8 ms since initial road contact

were kept constant and the shear stress limit at the head/liner interface reduced by a factor of 2.5, there was also little effect.

Helmets, designed for increased linear-deceleration protection, may not be ideal for protection against rotational acceleration. However, it is wrong to argue that a projecting part of a vehicle, by indenting the soft foam liner, will cause a large rotational moment on the head, hence a large rotational head acceleration. The moment is not large, because there is slip at the liner/head interface. For an oblique impact on the right 70° site on the road with $V_T = 10$ m/s, comparison of predictions for the S1 helmet (Table 5) and the thicker 16-hole helmet (Table 4) shows that the peak head rotational accelerations are similar, although the helmet liner thickness has changed.

4.3 Effective kinetic energy

Some experts evaluate the potential performance of a bicycle helmet (for a head-injured rider who did not wear a helmet) by estimating the total kinetic energy of the cyclist's head precrash. This would be reasonable if the head had made a direct (perpendicular) impact into an immovable, flat, rigid object. However this is extremely rare. Both FEA [**2**] and oblique impact tests [**2**] on bicycle helmets show that the peak linear headform acceleration is determined largely by the vertical component of head-to-road impact velocity, and is nearly independent of the horizontal velocity component. Hence, the total kinetic energy of the head prior to impact does not determine the peak linear head acceleration; the effective kinetic energy is that calculated from the velocity V_N alone.

4.4 How helmets limit head rotational acceleration

As discussed in section 2.8, impact forces cause both linear and rotational head acceleration. The crushing of the helmet liner prevents or reduces brain injuries by reducing the peak impact force F_N to less than 10 kN, thereby reducing the peak head accelerations. Assuming that the postimpact rebound velocity of

Downloaded from pil.sagepub.com at PENNSYLVANIA STATE UNIV on March 4, 2016

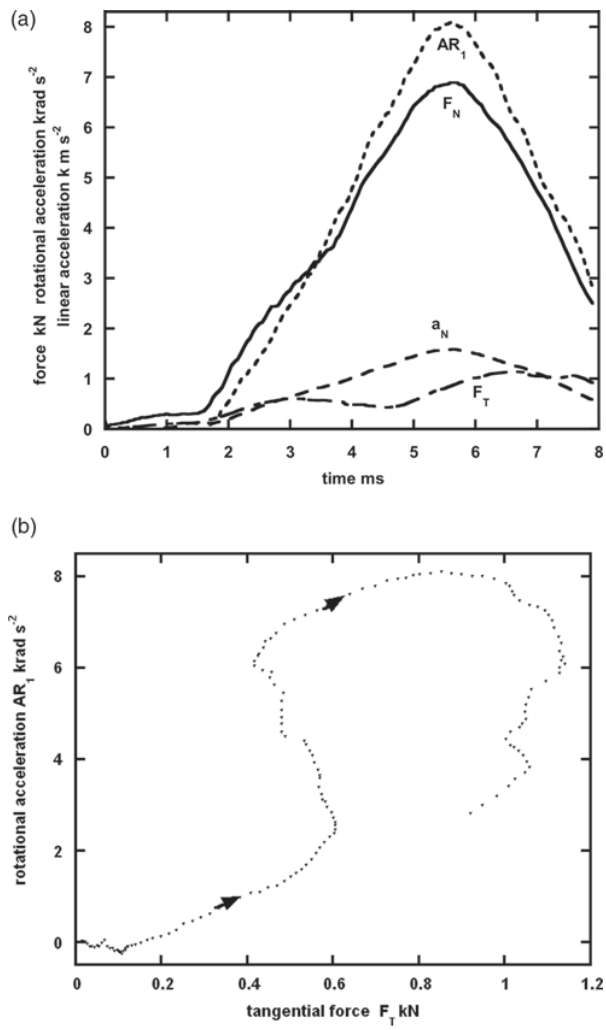

Fig. 5 For the simulation of Fig. 2: (a) road forces and headform accelerations versus time and (b) correlation of head rotational acceleration about the 1 axis, with the tangential force F_T

the head is small and not affected by the presence of the helmet, by Newtonian mechanics, the impulse required to change the head's momentum is the same. However, the crushing of the foam spreads the impulse over a longer time. In Fig. 6, the area

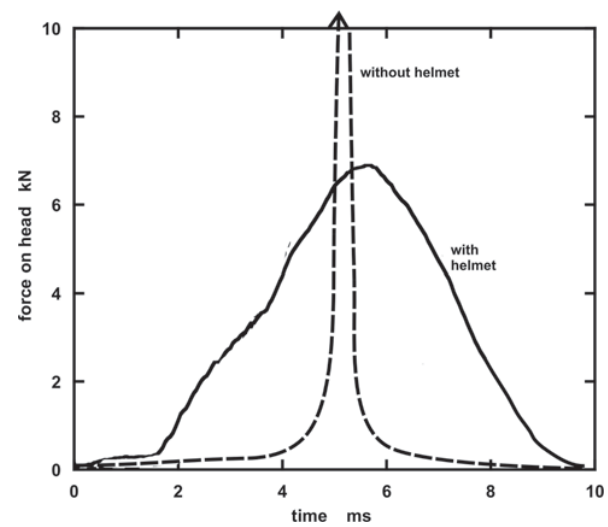

Fig. 6 Head impact force versus time trace with (based on FEA) and without (schematic) a helmet. The areas under the curves (the impulses) are the same

under the two graphs is the same, but there is a lower peak force with a helmet. Hence, liner crushing also reduces the peak rotational acceleration of the head.

To perform FEA of a bare head impacting a road, it would be necessary to model details of the skull geometry, so it is difficult to predict the 'no-helmet' curve in Fig. 6. Similarly, oblique impacts are not performed with a 1.5 m drop of a bare instrumented headform, because it would be damaged.

5 PROTECTING MORE OF THE TEMPLE AND FOREHEAD

5.1 Oblique impacts near the helmet lower edge

Head protection depends on whether the impact site is initially covered by the helmet and whether helmet rotation later in the impact allows a region of the skull to strike the road. Figure 7 compares lateral views of two helmets on an Ogle headform. The

Table 5 Peak headform accelerations, as a function of the friction coefficients, for impacts with $V_N = 5$ and $V_T = 10$ m/s on the right 70° site of the S1 helmet containing EPS 83 foam

Head/liner friction coefficient	Shell/road friction coefficient	Head a_{max} (g)	Head $\ddot{\theta}_1^{max}$ (k rad/s^2)	Head $\ddot{\theta}_2^{max}$ (k rad/s^2)	Head $\ddot{\theta}_3^{max}$ (k rad/s^2)
0.6	1.2	163	−8.0	−1.3	6.6
1.2	1.2	163	−8.1	−1.4	6.6
0.6	0.6	160	−7.9	−0.7	6.6
0.3	0.3	161	−7.5	−1.1	6.5
0.15	0.15	160	−7.2	−0.7	6.7

Downloaded from pil.sagepub.com at PENNSYLVANIA STATE UNIV on March 4, 2016

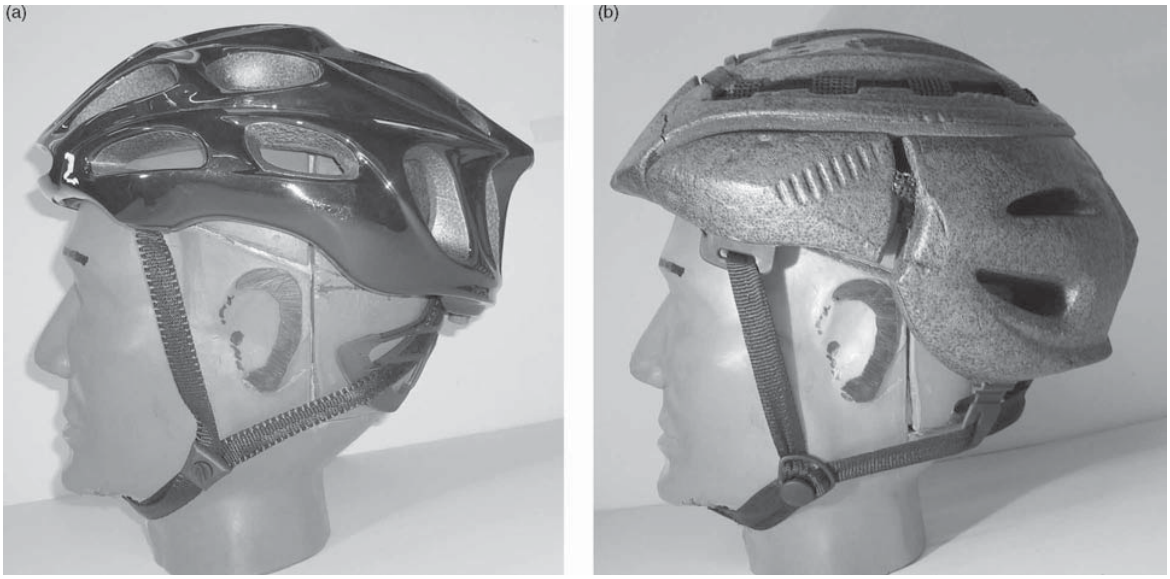

Fig. 7 Coverage of an Ogle headform: (a) S1 and (b) Sportcraft helmets

coverage of the specialized S1 helmet is less, exposing more of the vulnerable area above the ear. Peoplesize software (Open Ergonomics Ltd, Loughborough, Leics. UK) shows that the distance from the tragion (ear opening) to the crown of the head varies from 110 mm (5th percentile female adult) to 143 mm (95th percentile male adult). Since helmets appear to avoid covering the ear of the 5th percentile female, it is likely that a 95th percentile male could have a 30 mm gap between the top of his ear and the lower edge of the helmet.

Cycle helmets can be displaced on the head in an impact. Figure 8 compares FEA predictions for oblique impacts at the frontal 90° site, with velocity components $V_N = 5.4$ and $V_T = 5$ m/s. In principal, the tangential velocity V_T should cause the helmet to move down on the forehead. However, the shape of the S1 helmet interior causes it to move up on the forehead, allowing the forehead to strike the road 4.5 ms into the impact (Fig. 8(b)); the interaction of the lower jaw with the road was ignored. Only 25 J of kinetic energy were absorbed up to this point. In contrast, the 16-hole helmet, positioned further down the forehead with an inner surface more 'vertical' on the face (Fig. 8(c)), is predicted to move down over the face (Fig. 8(d)), adding to the protection of the forehead. In neither case does the retention system keep the helmet fixed in place, given the sliding at the 'hair' interface, and the motion of the chin straps around the face.

These predictions suggest that helmets with better coverage of the temple and forehead should be developed, and that standards should require (oblique) impact tests at the front edge of the helmet. The fit of a helmet to the range of head shapes and sizes becomes more difficult as greater amounts of the head are covered. A range of EPS liners would be necessary to fit the majority of head shapes in the population. It is not realistic to use thick layers of soft open-cell polyurethane 'comfort' foam as in motorcycle helmets. Semirigid foams could possibly be used in the temple region, allow greater coverage, while flexing to fit the head shape. However, foam at the side of the head could increase the thermal insulation of the head and, at the front, must not reduce the field of view of the cyclist.

5.2 The effects of head size

The trend to a single size helmet liner, with an adjustable headband, may have consequences for cyclists with small diameter heads. According to Ruan and Prasad [**27**], the concussion tolerance levels for adult heads of different sizes, expressed in terms of the head injury criterion (HIC), are almost the same. HIC is a time integral of the linear acceleration, raised to the 2.5th power. However, as Bosch *et al.* [**28**] point out, the head mass increases with the cube of its circumference. The head moments of inertia, which affect its angular acceleration, also increase with the cube of its circumference. Modelling of pressure waves in the brain in impacts [**29**] suggested that the peak pressures did not directly correlate with HIC when the head size was varied. Consequently, it is unclear whether the tolerances to peak linear or rotational accelerations are functions of head size.

Downloaded from pil.sagepub.com at PENNSYLVANIA STATE UNIV on March 4, 2016

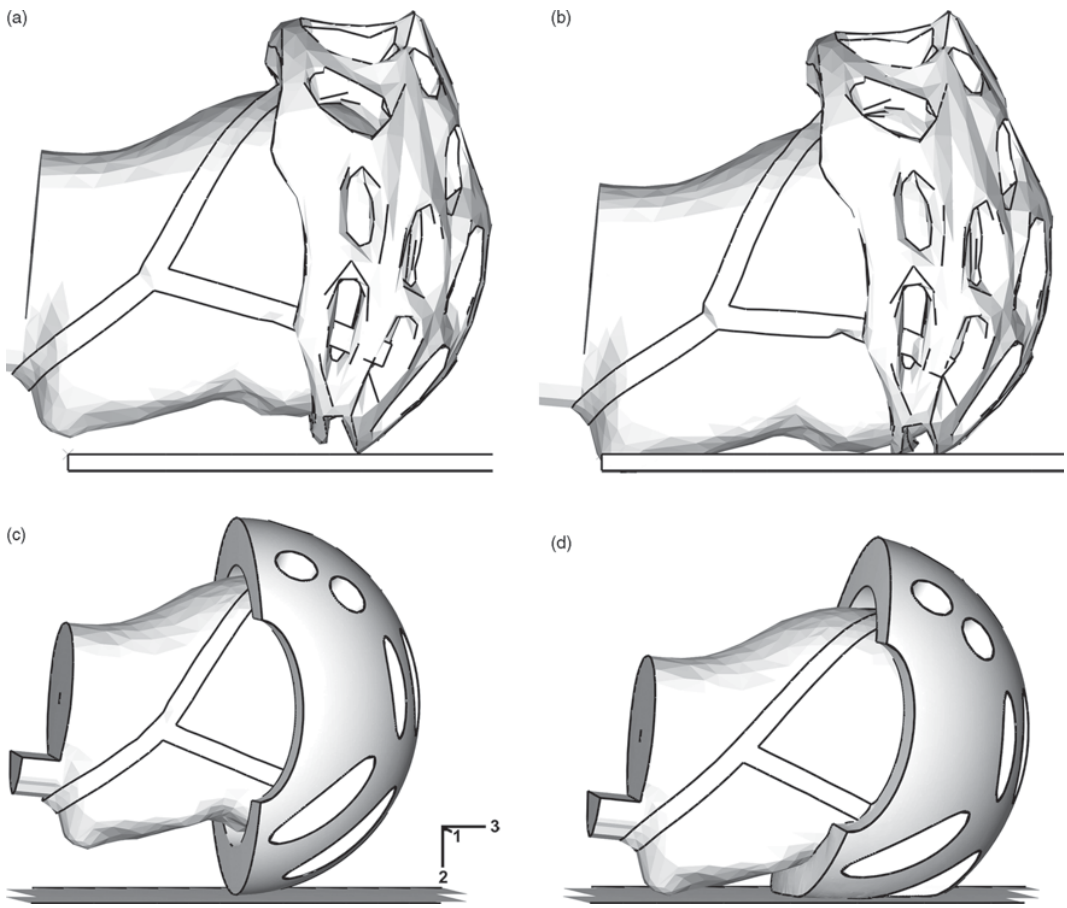

Fig. 8 FEA predictions for oblique impacts with $V_N = 5.4$ and $V_T = 5$ m/s at the frontal 90° site: (a) S1 helmet at initial contact, (b) after 3.2 ms, with forehead-to-road impact, (c) 16-hole helmet initially, and (d) after 8.4 ms

If the head's radius of curvature is significantly smaller than that of the helmet liner interior at the impact site, this should reduce the loading stiffness of the helmet liner. Several manufacturers use a single size liner, with an adjustable headband, to fit all head sizes (although specialized use different liner sizes in their helmets). FEA was used to model a headform of 10 per cent smaller dimensions, i.e. with circumference ~522 mm rather than the initial 580 mm, in the S1 helmet shape. The mass and moments of inertia were scaled by 0.9^3 so the mass is 3.1 kg (the mass of a 500 mm headform according to EN 960 for headforms). Figure 9 shows, for a side 70° impact site, the peak linear head acceleration was almost identical, at 171 g compared with 160 g for the headform of 580 mm circumference. However, the peak rotational acceleration about the 1 axis, at 4.75 k rad/s^2, was 40 per cent smaller for the smaller headform. Therefore, the engineering performance of 'one-size' helmets changes with headform size; human factors are likely to cause further variations in the injury levels experienced.

6 PROBLEMS WITH EXISTING HELMET FOAMS

6.1 Potential risk of skull fracture from high-density EPS foams

Although helmet liner densities have increased over the last 20 years, to compensate for the presence of large ventilation slots, this does not lead to pressures on the skull that will cause bruising or injury. Such vents improve head cooling, needed to make helmets acceptable to racing cyclists.

Figure 10 shows the predicted pressure distribution on a deformable headform with a S1 helmet containing EPS of density 83 kg/m^3. On the surface of the head, the pressure distribution follows the shape of the liner interior, for a contact area much greater than 5 cm^2. The maximum pressure was

Downloaded from pil.sagepub.com at PENNSYLVANIA STATE UNIV on March 4, 2016

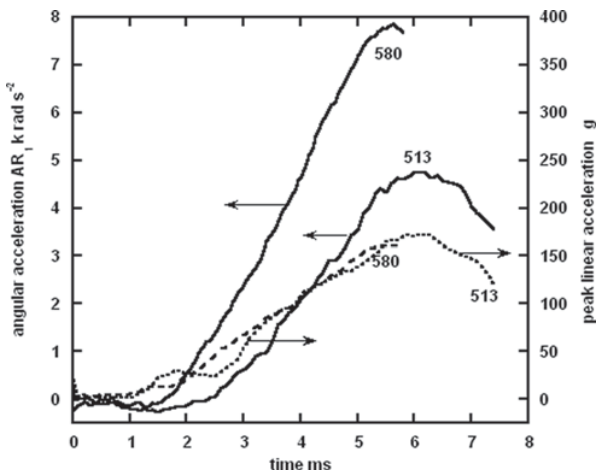

Fig. 9 Predicted time variation of accelerations for heads of 522 and 580 mm circumference in the S1 helmet: for oblique impacts with $V_N = 5.4$ and $V_T = 5$ m/s at the right 70° site

predicted to be 2 MPa at the peak of the simulation, a pressure that should not cause scalp bruising. It was not possible to evaluate the risk of skull fracture, since this would require a model with the full skull geometry and bone fracture strengths. However, the large area of load application shown in Fig. 10 is greatly preferable to the small area loaded when an unprotected skull hits the road. It is unlikely that any polymer foam based helmet would cause a skull fracture so long as the impact energy is within its capacity.

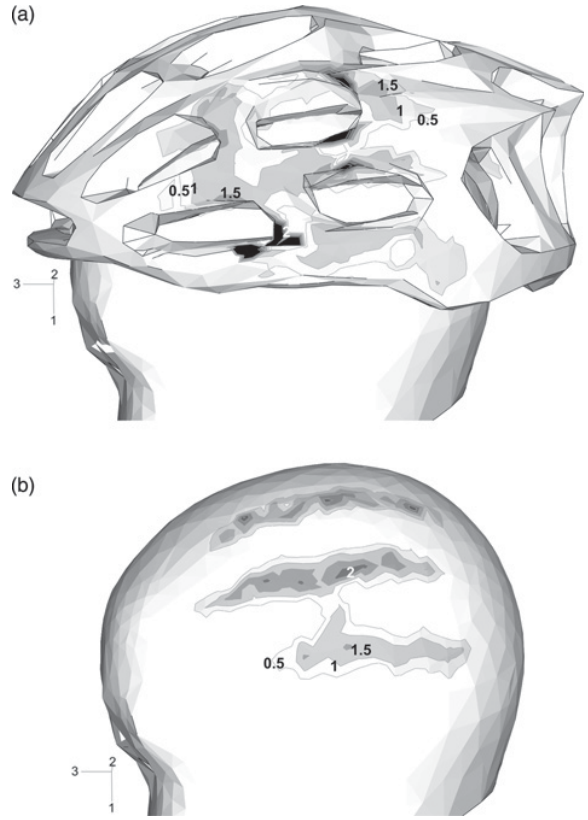

Fig. 10 Contours of pressure σ_{22} (MPa) after 5.0 ms of an oblique impact with $V_N = 5.4$ and $V_T = 4.0$ m/s at the left 70° site of a S1 helmet: (a) on the liner exterior and (b) on the deformable headform

6.2 Is the foam response non-ideal for head protection?

Both Fig. 2(b) and prior results [**2**, **3**] show that the impact force on helmets rises nearly linearly with the crushing of the liner foam, in spite of the foam having an initial yield stress. The linear increase in the road to helmet contact area with the foam crush distance leads to equation (5). When FEA was run for lower V_N values, the impact force is predicted to vary with liner crush in the same linear manner, so the peak impact force is linearly proportional to the normal component of the impact velocity. This refutes Burdett's claim that serious injuries can occur in minor crashes due to the impact force being just sublethal.

7 DISCUSSION

Comments [**5**, **7**] about helmets being ineffective if the impact velocity exceeds 20 km/h are misleading; 'velocity' should read 'velocity component, perpendicular to a rigid object'. The peak linear acceleration in an oblique impact test was predicted to be the same or less than that in a BSEN 1078 test, for the same velocity component perpendicular to the anvil. Consequently helmets, which meet BSEN 1078, should keep the head peak linear acceleration in oblique impacts at reasonable levels, so long as the impact site is one of those tested in the standard. Even for impacts with a high normal velocity V_N, the simulated specialized helmet absorbs ~100 J of the impact energy before the liner bottoms out; therefore, 100 J less impact energy is transmitted directly to the skull through a small contact area of fully compressed foam. This must reduce the severity of the head injuries compared with not wearing a helmet. Helmets are likely to prevent head injuries unless the cyclist's head strikes either a moving vehicle, or vertical street furniture, with an excessive velocity. In special circumstances, a cyclist's head may undergo a high rotational acceleration; if a cyclist rides across the path of a fast moving car and their head impacts the car windscreen, the

Downloaded from pil.sagepub.com at PENNSYLVANIA STATE UNIV on March 4, 2016

windscreen fractures. The cyclist's body goes either to the side of, or over the top of, the car, and the cyclist's head is suddenly withdrawn from the broken windscreen. Therefore, helmets are not necessarily effective at preventing head injury in all circumstances.

Committees responsible for bicycle helmet standards should encourage increases in protection levels. However, such increases in other standards are thought to have unintended effects. A review of motorcycle helmet design [**30**] criticized the effects of the Snell standard (which has higher impact energies than other US standards) on the type of helmet being bought in the USA. The authors were concerned about increased purchases of Snell-certified helmets, because of their high density liners. Although they might benefit the small fraction of motorcyclists involved in high velocity crashes, their design was felt to be suboptimal for the average impact velocity. A similar situation should be avoided for bicycle helmets. Rather than just increasing the impact energy, it would be beneficial to reduce the peak linear acceleration level in the standard from 250 g towards 150 g (the approximate equivalent of the HIC allowed in car occupant testing).

Although frontal impact sites are common in real crashes, in BSEN 1078 direct impact are restricted to sites that lie above the equivalent of the frontal 80° site. This may be to avoid damage to the headform from contacting the anvil, or possibly the lower performance of helmets at the frontal site. Oblique impacts allow testing the frontal 90° site. As helmets vary in the liner thickness, coverage, and shape at this site, and in the ventilation hole size, their performance is likely to vary (as shown in Fig. 9), and the best designs should be encouraged. An oblique impact test in BSEN 1078 would also encourage the development of designs which minimize head rotational acceleration.

Future modelling of helmet performance should use realistic skull models, with failure criteria for the bone. Skull fracture has been modelled for an impact without a helmet [**31**], but not for an impact with a helmet. The modelling relies on old data for bone fracture stresses. Given the variation in skull thickness, both site to site and person to person, this is likely to be a complex area.

8 CONCLUSIONS

Helmet protection levels can be increased, through the use of thicker helmet liners of lower density EPS. This may involve the redesign of cooling vents, to avoid unstable deformation modes. No currently available materials are significantly superior to EPS for use as the helmet liner. FEA does not suggest any particular advantage in the use of dual density helmet liners.

The peak head rotational acceleration, in typical oblique impacts with the road, is typically insufficient to risk rotational brain injuries. It is unlikely to be significantly decreased by the use of a low-friction external layer on the helmet shell.

The coverage of the forehead and temples could be improved with some reduction of head cooling. Impact tests on frontal sites are needed, both because of the frequency of such sites in crashes and because helmet performance is likely to vary considerably.

ACKNOWLEDGEMENT

The authors thank EPSRC for support under grant R89790.

REFERENCES

1 **Aldman, B., Lundell, B.,** and **Thorngren, L.** Oblique impacts – a parametric study in crash helmets. IRCOBI Conference, Lyon, 1978, p. 129.
2 **Gilchrist, A.** and **Mills, N. J.** Dynamic FEA of bicycle helmet oblique impacts. *Int. J. Impact Eng.*, 2006, submitted for publication.
3 **Gilchrist, A.** and **Mills, N. J.** Oblique impact testing of bicycle helmets. *Int. J. Impact Eng.*, 2006, submitted for publication.
4 **BSEN 1078.** *Helmets for pedal cyclists and for users of skateboards and roller skates*, 1997 (BSI, London).
5 **Henderson, M.** The effectiveness of bicycle helmets: a review, report for Motor Accidents Authority of New South Wales, 1995, available from www.bhsi.org/webdocs/.
6 **McIntosh, A.** and **Dowdell, B.** A field and laboratory study of the performance of pedal cycle helmets in real accidents. IRCOBI Conference, 1992, pp. 51–60.
7 **British Medical Association**. *Cycle helmets*, 1999 (BMA, London).
8 **Mills, N. J.** *Plastics: microstructure and engineering applications*, 3rd edition, 2005 (Butterworth Heinemann, London).
9 **Williams, G. J.** *Protective Helmet*, US patent 6070271, 2000.
10 **Mills, N. J.** and **Hwang, A. M.** The multi-impact performance of high-density polyethylene foam. *Cell. Polym.*, 1989, **8**, 259–276.
11 **Loveridge, P.** and **Mills, N. J.** The mechanism of recovery of impacted high-density polyethylene foam. *Cell. Polym.*, 1991, **10**, 393–405.
12 **Halldin, P., Gilchrist, A.,** and **Mills, N. J.** A new oblique impact test for motorcycle helmets. *Int. J. Crash.*, 2001, **6**, 53–64.
13 **Harrison, A., Mills, N. J.,** and **Turner, J. M.** Jockeys' head Injuries and skull cap performance. IRCOBI Conference, Dublin, 1996, pp. 49–62.
14 **Phillips, K. D.** *Protective headgear and protective armour*. WO 03/005844 A1 patent, 2003.

Downloaded from pil.sagepub.com at PENNSYLVANIA STATE UNIV on March 4, 2016

15 **Gennarelli, T. I.** and **Thibault, L. E.** Clinical rationale for a head injury angular acceleration criterion. *Head Injury Mechanisms*, 1989, pp. 5–8 (AAAM, Washington).

16 **Depreitere, B., van Lierde, C., Maene, S., Plets, C., van der Sloten, J., van Audekercke, R., van der Perre, G.,** and **Goffin, J.** Bicycle-related head injury: a study of 86 cases. *Accid. Anal. Prev.*, 2004, **36**, 561.

17 **BS 6863** *Pedal cyclists' helmets*, 1987 (British Standards Institution, London).

18 **Yoganandan, N., Zhang, J.,** and **Pintar, F. A.** Force and acceleration corridors form lateral head impact. *Traffic Inj. Prev.*, 2004, **5**, 368–373.

19 **Watters, R. D., Tutton, J. C., Balatti, A. F., Fletcher, M. A., Shewchenko, N., Bayne, T. D.,** and **Withnall, C. R. P.** (*Sportcraft*) *Insert-molded helmet*, US patent 6292952, 2001.

20 **Burdett, A.** Frequently asked questions. (Ocbc = Ontario Coalition for Better Cycling), 2002, available from www.magma.ca/~ocbc.

21 **Aldman, A.** A method for the assessment of the load distributing capacity of protective helmets, Chalmers University of Technology, Goteborg, 1984.

22 **Thompson, D. C., Rivara, F. P.,** and **Thompson, R.** Helmets for preventing head and facial injuries in Bicyclists, The Cochrane Library, Issue 1, Oxford, 2003.

23 **Curnow, W. J.** The efficacy of bicycle helmets against brain injury, *Accid. Anal. Prev.*, 2003, **35**, 287–292.

24 **Masso-Moreu, Y.** and **Mills, N. J.** Impact compression of polystyrene foam pyramids. *Int. J. Impact Eng.*, 2003, **28**, 653–676.

25 **Masso-Moreu, Y.** *Study of protective packaging materials*. PhD thesis, University of Birmingham, 2005.

26 **Mills, N. J.** and **Gilchrist, A.** Properties of bonded polypropylene bead foams. *J. Mater. Sci.*, 2006, submitted for publication.

27 **Ruan, J. S.** and **Prasad, P.** On the consequence of head size following impact to the human head. *J. Biomech.*, 2006, **39**, 383–385.

28 **van der Bosch, E., Leensen, M. W. B. M., Klomp, N. H. M., Sauren, A. A. H. J.,** and **Wismans, J. S. H. M.** Development of an improved dummy head for use in helmet certification tests, Proceedings of ASME Symposium on *Crashworthiness*, Orlando, 2000, 17 pp.

29 **Kleiven, S.** and **van Holst, H.** Consequences of head size following trauma to the human head. *J. Biomech.*, 2002, **35**, 153–160.

30 **Ford, D.** Blowing the lid off. *Motorcyclist Mag.*, June 2005.

31 **Willinger, R.** and **Baumgartner, D.** Human head tolerance limits to specific injury mechanisms. *I. J. Crash.*, 2003, **8**, 605–617.

APPENDIX

Notation

a	acceleration
F	force
I	moment of inertia
L	length
m	mass
p	hydrostatic pressure
p_c	yield pressure in compression
p_t	yield pressure in tension
R	foam relative density
R_H	helmet radius
V	velocity
x	distance
ε	strain
$\ddot{\theta}$	rotational acceleration
σ_C	uniaxial compression yield stress
σ_y	yield stress

Downloaded from pil.sagepub.com at PENNSYLVANIA STATE UNIV on March 4, 2016